Nano Carbons 2024; 2(1): 298.
Original Research Article

The study of multilayer graphene membrane performance in O_2 purification process: Molecular dynamics simulation

Mohammad Pour Panah[1], Bahman Parvandar Asadollahi[2], Roozbeh Sabetvand[3,*]

[1] *Department of Physics, Faculty of Basic Sciences, Tarbiat Modares University, Tehran 14115-111, Iran*

[2] *Mechanical Engineering Department, Faculty of Engineering, Shahid Chamran University of Ahvaz, Ahvaz 61357-83151, Iran*

[3] *Department of Energy Engineering and Physics, Faculty of Condensed Matter Physics, Amirkabir University of Technology, Tehran 159163-4311, Iran*

*** Corresponding author:** Roozbeh Sabetvand, r.sabetvand@gmail.com

ARTICLE INFO

Received: 9 November 2023
Accepted: 26 February 2024
Available online: 9 April 2024

doi: 10.59400/n-c.v2i1.298

ABSTRACT: We use molecular dynamics (MD) method to describe the atomic behavior of Graphene nanostructure for Oxygen molecules (O_2) separation from Carbon dioxide (CO_2) molecules. Technically, for the simulation of graphene-based membrane and O_2-CO_2 gas mixture, we used Tersoff and DREIDING force fields, respectively. The result of equilibrium process of these structures indicated the good stability of them. Physically, this behavior arises from the appropriate MD simulation settings. Furthermore, to describe the purification performance of graphene-based membrane, we report some physical parameters such as purification value, impurity rate, and permeability of membrane after atomic filtering process. Numerically, by defined membranes optimization, the purification value of them reach to 97.31%. Also, by using these atomic structures the CO_2 impurity which passed from graphene-based membrane reach to zero value.

KEYWORDS: graphene; atomic membrane; molecular dynamics; purification process; oxygen; carbon dioxide

1. Introduction

Atomic membranes are a new class of low-dimensional, free standing, physically stable, and virtually impermeable materials[1–4]. The common 2D atomic membrane is graphene nanosheet, a two-dimensional lattice entirely made of carbon atoms, but other interesting structures such as the multilayer graphene offer new properties[5–8]. Structurally, graphene nanosheet is a layer of carbon atoms which are bonded together with covalent interaction in honeycomb lattice. This atomic structure shows promising properties including a high specific surface area, good thermal conductivity, proper mechanical behavior, and excellent charge mobility[9,10]. Due to these interesting properties, this atomic layer has remained at the core of scientific research since its advent, with many of its successful accomplishments being transformed into various applications. Today, graphene-based nanostructures are used commonly in fuel cells[11,12], supercapacitor[13,14], capacitive deionization[15–17], desalination[18–20]. Furthermore, graphene-based membranes are the other class of this atomic structure applications. These atomic membranes are capable of creating an appropriate barrier when dealing with liquids and gasses particles. Graphene-based membranes effectively separate target atoms from liquid and gasses environment. Physically, due to the repulsive interaction of the π-bond orbital electron distrobution in graphene nanosheet, this atomic structure is not permeable to liquid or gas environment[21].

These practical properties of graphene membrane can be studied with experimental and theoretical approaches. Molecular Dynamics (MD) method is one of the important methods in the atomic study of various nanostructures[22–25]. Previously, this computational method used for graphene-based membrane study. Cohen-Tanugi and Grossman[26] showed that nanoporous graphene membranes can remove NaCl from H_2O molecules. In their work, simulation results show the single layer membranes delivery capacity reach to 66 L/(cm²·day·MPa). In other work, this research group used single layer graphene as a reference structure to explore the possibility of multilayer graphene membranes[27]. The result of this computational work show the appropriate properties of multilayer grapgene structures as atomic membrane. Kim et al.[28] described the transport of H_2O molecules and atomic ions in the pores of the graphene nanosheet. The MD results indicated the use of hydroxylated graphene pores can improve the membrane efficiency for actual applications. Also, Wang et al.[29] used graphene nanosheet on polyacrylonitrile matrix to introduce an effective graphene oxide membrane. It was found that with graphene oxide thickness increasing, the H_2O molecules flux decreased appreciably. So, due to the appropriate performance of MD simulations in the study of graphene-based membranes behavior, in this work we use of this approach to describe of multilayer (3-layers) graphene membrane performance in O_2 purification process from O_2-CO_2 gas mixture for the first time. In our MD simulations, the distance between various sheets and porous radius changes to designing optimized atomic membrane for O_2 molecules purification process to actual applications.

2. Computational method

In this MD study, graphene membrane and initial mixture gas (O_2-CO_2) interact with each other for the t = 2 ns. This atomic procedure determines the graphene membrane filtering performance in O_2 purification process. In our computational approach, simulations were done by LAMMPS package[30–33]. By using this computational package, multi-layer graphene membrane and O_2-CO_2 gas mixture simulated as C, H, and O atoms arrangement as depicted in **Figure 1**. This atomic structure depicted by OVITO (Open Visualization Tool) software[34]. Computationally, in depicted atomic structures, fix boundary conditions were used in x direction and periodic style implemented to y and z directions[35]. After atomic modeling, NVT ensemble used in our MD simulations to equilibrate the temperature of structures[36,37]. This computational ensemble equilibrate the modeled samples at T_0 = 300 K with 0.001 damping value for temperature.

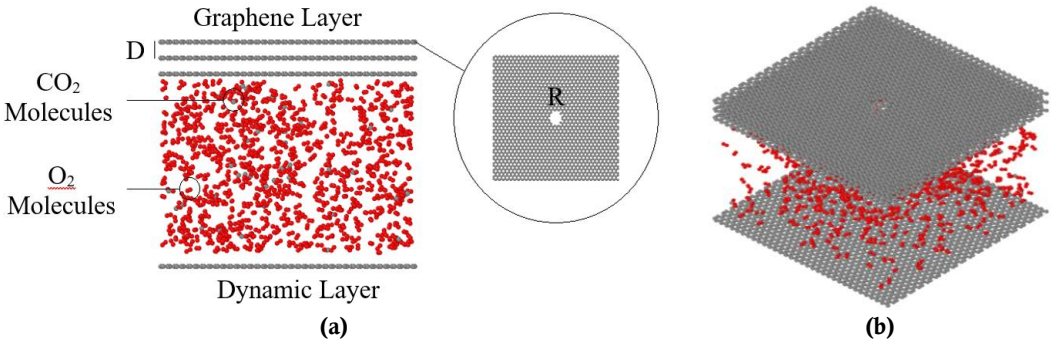

Figure 1. Multi-layer graphene membrane and O_2-CO_2 gas mixture simulated as C, H, and O atoms arrangement. **(a)** atomic properties of simulated structures with LAMMPS package; **(b)** atomic structures arrangement inside MD simulation box.

Atomic force-field is an important parameter in common MD simulations. To simulate the atomic structures inside MD box, we use DREIDING and Tersoff force-fields[38,39]. In DREIDING force-field, the atomic interactions were presented by non-bonded and bonded terms. The non-bond term in atomic

structures simulation defined by the Lennard-Jones (LJ) equation (12-6 type) as reported in Equation (1). Historically, this mathematical function was introduced by John Lennard Jones for the first time as Equation (1)[40]:

$$E(r) = 4\varepsilon\left[\left(\frac{\sigma}{r_{ij}}\right)^{12} - \left(\frac{\sigma}{r_{ij}}\right)^{6}\right], \qquad r \ll r_c \tag{1}$$

In Equation (1), ε is the depth of the potential well, σ is the distance at which the potential function is zero and r_{ij} is the atomic distance. These physical parameters selected with type of atoms in simulated structures. So, these parameters value for all atoms in our MD simulation reported in **Table 1**[39].

Table 1. The ε and σ constants for LJ interactions in our MD simulation box[39].

Type of atoms	σ (Å)	ε (kcal/mol)
C	4.180	0.3050
H	3.200	0.0100
O	3.710	0.4150

The bonded term of atomic interactions consists of simple and angle strengths. The bond and angle strengths in DREIDING force-field is calculated by harmonic oscillator formalism as Equations (2) and (3), respectively[39]:

$$E_r = \frac{1}{2}k_r(r - r_0) \tag{2}$$

$$E_\theta = \frac{1}{2}k_\theta(\theta - \theta_0) \tag{3}$$

In Equations (2) and (3), K_r and K_θ are the constants of harmonic oscillator. Also, r_0 and θ_0 are the equilibrium value of bond length and angle, respectively. Harmonic oscillator constants (K_r and K_θ) in DREIDING force-field set to 700 (kcal/mol)/ Å^2 for each atomic bond and 100 (kcal/mol)/degree^2 for all bond angle bend. Furthermore, the equilibrium value of bond length and angle in our simulated structures listed in **Table 2**[39].

Table 2. The r_0 and θ_0 values for the bond strength and angle bend of simulated structures by MD method[39].

Parameter	r_0 (Å)	θ_0 (degree)
C-O bond	1.420	-
O-O bond	1.310	-
O-C-O angle	-	109.471

As mentioned before, Tersoff force-field used for C atoms interaction in graphene nanosheets as below[38]:

$$E = \frac{1}{2}\sum_i \sum_{j \neq i} E_{ij} \tag{4}$$

$$E_{ij} = f_C(r_{ij})[f_R(r_{ij}) + b_{ij}f_A(r_{ij})] \tag{5}$$

where f_R is a two-body term and f_A include three-body interactions. The summations in Equation (5) are over all neighbors j and k of atom i within a cutoff radius. After defining an appropriate force-field to O_2-CO_2 gas mixture and graphene-based membrane, MD study was fulfilled. Then, to describe the atomic structures time evolution inside MD box, Newton's law's is used as the gradient of selected force-fields[35]:

$$F_i = \sum_{i \neq j} F_{ij} = m_i \frac{d^2 r_i}{dt^2} = m_i \frac{dv_i}{dt} \quad (6)$$

$$F_{ij} = -\nabla V_{ij} \quad (7)$$

From these base equations, the atomic momentum P_i can be defined as Equation (8)[37]:

$$P_i = m_i v_i \quad (8)$$

In the stated equations, to integrate the Newton's law's, the association of equation (6) is done by the Velocity-Verlet algorithm as below[35]:

$$r(t + \delta t) = r(t) + v(t)\delta t + \frac{1}{2} a(t)\delta t^2 \quad (9)$$

$$v(t + \delta t) = v(t) + \frac{1}{2}[a(t) + a(t + \delta t)]\delta t \quad (10)$$

In Equations (9) and (10), $r(t + \delta t)$, $v(t + \delta t)$is the position and velocity of atoms in $t + \delta t$ and $r(t)$, $v(t)$ is the value of these physical quantities in t. Furthermore, in MD simulation approach, Gaussian distribution is implemented for temperature calculating in atomic arrangement as Equation (11)[35]:

$$\frac{3}{2} k_B T = \frac{1}{N_{atom}} \sum_{i=1}^{N} \frac{1}{2} m v_i^2 \quad (11)$$

Finally, the instantaneous temperature variation is calculated from Equation (12)[35]:

$$T(t) = \sum_{i}^{N} \frac{m_i v_i^2(t)}{k_B N_{sf}} \quad (12)$$

where, N_{sf} is the degree of freedom of the atomic systems. According to the reported descriptions, MD simulations in current computational study carried out as below:

- Step 1: CO_2-O_2 gas mixture and graphene-based membrane was simulated with DREIDING and Tersoff force-fields and equilibrated by NVT ensemble for 1,000,000 time steps with Δt = 1 fs. For this purpose, atomic structures temperature set at T_0 = 300 K as initial condition. After, atomic structures reached to equilibrium phase, the stability of them reported by temperature and potential energy calculating.
- Step 2: Next, atomic purification process settings implemented to equilibrated structures for 1,000,000 time steps with NVE ensemble (t = 1 ns). For this purpose, dynamic graphene sheet displaces in MD simulation box with constant velocity (see **Figure 2**). After this process, physical parameters such as: purification and permeability values reported to describe the atomic behavior of graphene-based membrane in O_2 purification process.

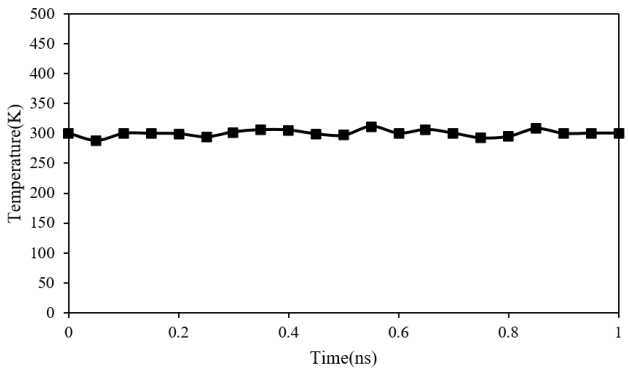

Figure 2. Temperature changes of graphene membrane and CO_2-O_2 gas mixture as a function of MD simulation time.

3. Results and discussion

3.1. Equilibration process of atomic structures

In the first step of our computational work, the atomic behavior of O_2-CO_2 gas mixture and graphene-based membrane was studied at initial temperature (T_0 = 300 K) for 1 ns. Our simulation results, showed the initial arrangement of particles in simulation box adopted with DREIDING and Tersoff force-fields[38,39]. This atomic phase of simulated structures reported by temperature and potential energy calculations. The simulated structures temperature changes as a function of simulation time as depicted in **Figure 2**. From calculated results, we conclude the atomic structures equilibrated after 1,000,000 time steps (t = 1 ns). Physically, this thermal equilibrium arises from atomic oscillation reducing which indicted our MD simulation settings validity[35]. Also, **Figure 3** shows the potential energy changes in atomic systems as a function of MD simulation time in this computational step. From this figure, we conclude the simulated structures potential energy converged after 1,000,000 time steps to constant value. Numerically, potential energy of graphene membrane and CO_2-O_2 gas mixture reached to −399 eV after 1 ns. Theoretically, this physical parameter has reciprocal relation by mean distance of atoms. By increasing the potential energy magnitude, the atomic stability of target system increased. **Figure 3** indicated, by increasing the initial porous radius (R) from 3 Å to 5 Å and 7 Å, the atomic system doesn't disrupted and so, stable phase of them can be detected after equilibrium process. Our calculations show the temperature of equilibrated structures reach to 300 K in the final step of simulations. Physically, atomic stability of initial membrane decreases by porous radius increasing. Numerically, by porous enlarging, the magnitude of potential energy parameter decreases to −376.81 eV from −406.69 eV. This behavior arises from carbon atom missing in membrane structure and interatomic force (by attraction type) decrease in defined layer system. Atomic layer distance between graphene sheets (D) is another important parameter for graphene-based membrane stability. By this parameter changes from 5 Å to 7.5 Å and 10 Å, the potential energy of the total atomic system decreases to −402.70 eV and −397.97 eV, respectively. This behavior arises from mutual interaction between carbon atoms which cause saving energy in MD simulation box. We can say the atomic stability of simulated membrane decreased by these potential energy's magnitude decreasing.

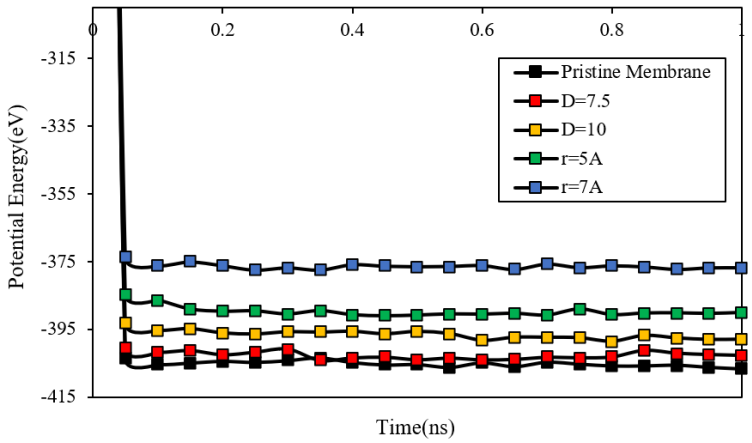

Figure 3. Potential energy changes of graphene membrane and CO_2-O_2 gas mixture as a function of porous radius and atomic layers distance.

3.2. Atomic behavior of simulated structures

3.2.1. Atomic behavior of pristine graphene membrane

In this step, MD settings implemented to pristine graphene membrane to study of O_2 molecules purification efficiency with this atomic arrangement. **Figure 4** shows the evolution of atomic structures after 320,000 time steps (t = 0.32 ns). After the equilibration phase, the number of filtered O_2 molecules variation as a function of MD simulation time reported in **Figure 5**. From this computational result, we conclude the MD simulation time (t = 1 ns) is long enough to the atomic purification process detecting. After this atomic phase, the number of CO_2 molecules which passed from graphene membrane reported (see **Figure 6**). From our MD simulation results, the number of filtered O_2 molecules reach to 603 (90.00% ratio) which this calculated value comparable with previous reports[41,42]. Also computed value of CO_2 molecules which passed from pristine membrane is 11 molecules (15.71% ratio). Reported atomic behavior of simulated structures in this MD simulation step show the validity of our computational settings and show the appropriate behavior of graphene-based membranes in atomic purification process.

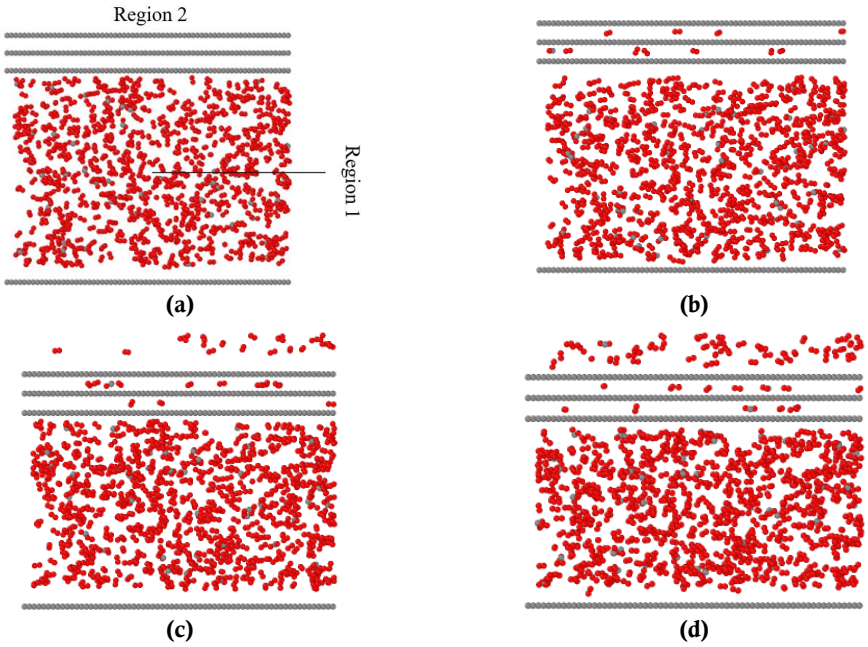

Figure 4. Time evolution of O_2-CO_2 gas mixture purification process with pristine graphene membrane. **(a)** t = 0; **(b)** t = 0.1 ns; **(c)** t=0.2 ns; **(d)** t = 0.3 ns.

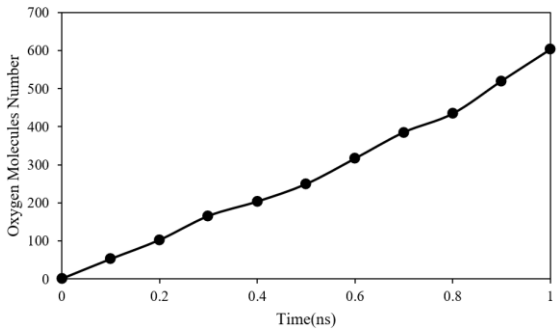

Figure 5. Number of O_2 molecules which passed from pristine graphene membrane as a function of MD simulation time.

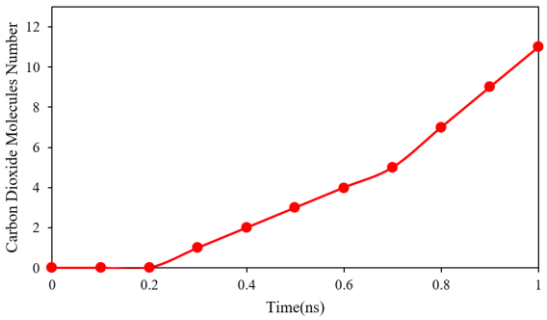

Figure 6. Number of CO_2 molecules which passed from pristine graphene membrane as a function of MD simulation time.

3.2.2. Graphene layers distance effect on atomic behavior of membrane

The results of graphene layers distance effects on carbon-based membrane purification behavior reported in this section of our MD study. The distance of atomic layers (D) which depicted in **Figure 1** are set to 5 Å, 7.5 Å, and 10 Å in NVT ensemble by setting initial temperature in T_0 = 300 K. After atomic equilibration process simulation for 1,000,000 time steps (t = 1 ns), the atomic structure were used for atomic purification process to estimate efficiency of them in this performance. Numerically, by D parameter increasing, the number of O_2 molecules which passed from carbon-based membrane decreases to 498 molecules (74.33% ratio) as reported in **Figure 7**. Furthermore, the CO_2 molecules elimination rate improve by D parameter increasing in modeled atomic membrane and the number of CO_2 molecules in region 2 reach to zero after 1 ns as depicted in **Figure 8**. Physically, by graphene layers distance variation, the attraction force which implemented to O_2-CO_2 gas mixture changes. This type of atomic interaction decreases by D parameter increasing and so the efficiency of graphene membrane improved. Also, the permeability of atomic structures affected by D parameter variation. From **Figure 9a** we can say the maximum value of this physical parameter reach to 62 L/cm^2/day/MPa and 43 L/cm^2/day/MPa by D parameter increasing from 7.5 Å to 10 Å, respectively. Here, the interaction energy between membrane atoms and gas mixture reported for more description of detected atomic phenomenon. This physical parameter indicated the atomic evolution of simulated structures. We report the total component of interaction energy in **Figure 9b**. MD results show that by D parameter enlarging, the interaction energy between membrane and O_2-CO_2 system decreases. This behavior arises from atomic distance increasing between simulated components which by this atomic evolution the membrane efficiency decreases. As reported in **Figure 9b**, D parameter enlarging cause interaction energy changes from −41.32 eV to −32.09 eV. By data analyzing from this section of our MD simulations, we conclude the D parameter increasing, improve the accuracy of atomic purification process and decreases the speed of this atomic phenomenon (as listed **Table 3**).

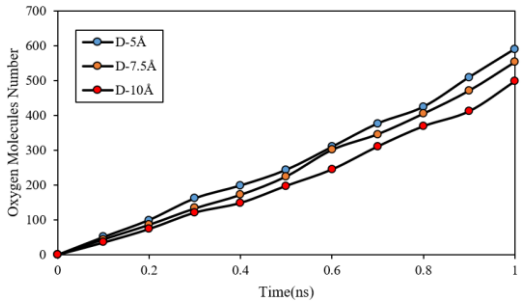

Figure 7. Number of O_2 molecules which passed from pristine graphene membrane as a function of graphene layers distance (D). The total number of O_2 molecules inside MD box is 670 molecules.

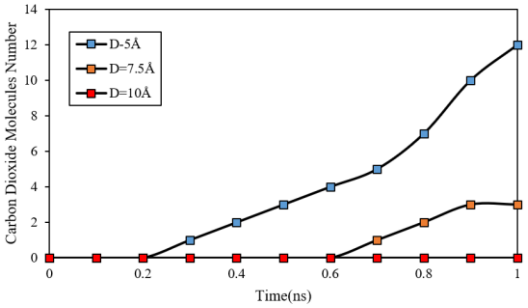

Figure 8. Number of CO2 molecules which passed from pristine graphene membrane as a function of graphene layers distance (D). The total number of CO_2 molecules inside MD box is 70 molecules.

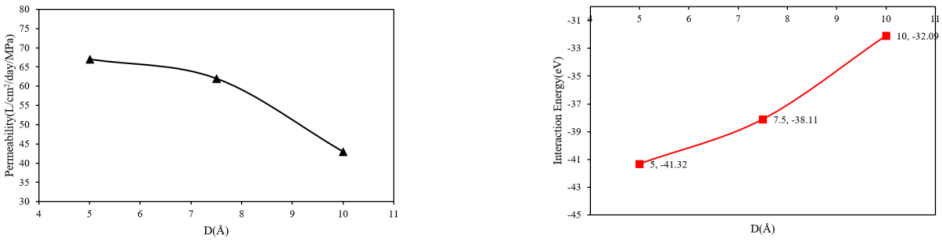

(a) **(b)**

Figure 9. (a) permeability of graphene-based membrane as a function of graphene layers distance (D); **(b)** interaction energy between atomic membrane and gas system as a function of D parameter.

Table 3. Number of O_2 and CO_2 molecules which passed from graphene-based membrane and membrane permeability as a function of graphene layers distance (D).

Graphene layers distance (Å)	Number of passed O_2 molecules	Number of passed CO_2 molecules	Permeability (L/cm²/day/MPa)
5	591	12	67
7.5	553	3	62
10	498	0	43

3.2.3. Graphene layers porous size effect on atomic behavior of membrane

In the final step of our computational work, we reported the graphene layers porous size (R) effect on carbon-based membrane purification efficiency. The porous size of graphene sheets set to 3 Å, 5 Å, and 7 Å at T_0 = 300 K. After MD equilibration process implementing for t = 1 ns, the dynamic graphene sheet move by 1 MPa pressure and so atomic purification process fulfilled after 1 ns. Our MD simulation results show that, by R parameter increasing, the number of O_2 molecules in region 2 increases from 591 molecules (88.21%) to 623 (92.98%) and 652 (97.31%) molecules (respectively) as reported in **Figure 10**. Furthermore, the CO_2 molecules elimination rate getting worse by R parameter increasing in graphene nanosheets. Numerically, CO_2 molecules elimination reach to 24.28% and 32.86% after 1 ns as depicted in **Figure 11**. Physically, by graphene layers porous size increasing, the atomic interaction between carbon atoms in membrane structure and O_2-CO_2 gas mixture decreased and the more molecules can be passed from graphene configuration as target membrane. The permeability of graphene membrane also affected by R parameter variation and the maximum value of this atomic separation factor reach to 71 L/cm²/day/MPa and 77 L/cm²/day/MPa (see **Figure 12a**). As previous section, interaction energy between atomic membrane and atomic gas mixture reported in **Figure 12b**. MD outputs in this section indicated the interaction energy get to more values by R parameter enlarging. By this process occur, the number of atoms which attracted by graphene sheets increased and number of passed molecules from target membrane improved. From these calculated

results, we can conclude R parameter increasing, decrease the accuracy of purification process and increase the speed of this atomic phenomenon as reported in **Table 4**.

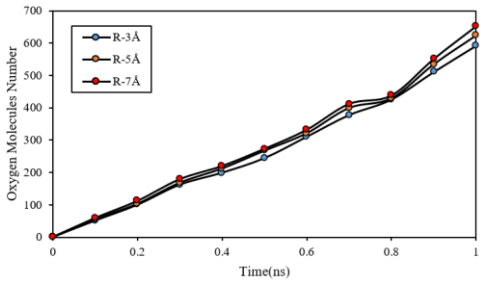

Figure 10. Number of O_2 molecules which passed from pristine graphene membrane as a function of graphene layers porous size (R).

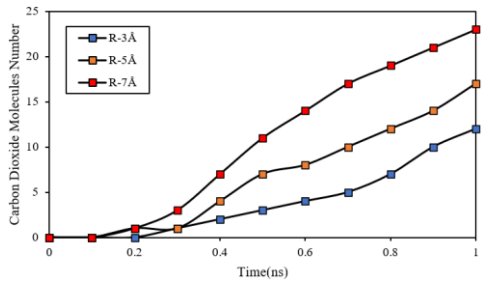

Figure 11. Number of CO_2 molecules which passed from pristine graphene membrane as a function of graphene layers porous size (R).

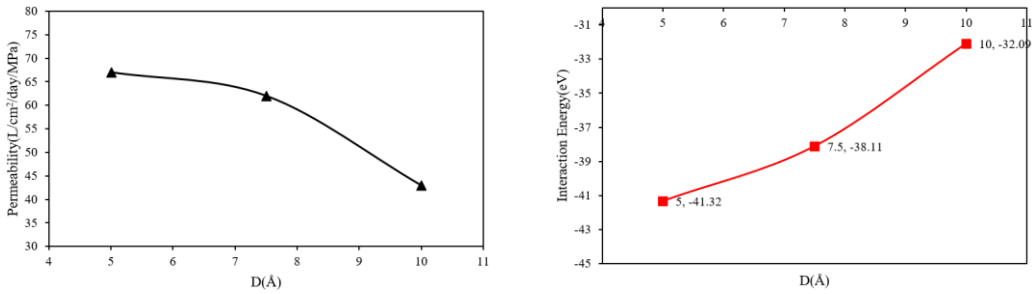

(a) **(b)**

Figure 12. (a) Permeability of graphene-based membrane as a function of graphene layers porous size (R); **(b)** interaction energy between atomic membrane and gas system as a function of R parameter.

Table 4. Number of O_2 and CO_2 molecules which passed from graphene-based membrane and membrane permeability as a function of graphene layers porous size (R).

Graphene layers porous size (Å)	Number of passed O_2 molecules	Number of passed CO_2 molecules	Permeability ($L/cm^2/day/MPa$)
3	591	12	67
5	623	17	71
7	652	23	77

4. Conclusion

We use Molecular Dynamics (MD) simulations to describe the behavior of multilayer (3-layers) graphene membrane in gas mixture purification process (O_2 molecules purification from O_2-CO_2 gas system). Our important computational results from MD simulations are as following:

- DREIDING and Tersoff force-fields are appropriate functions to MD simulation of graphene-based membrane and O_2-CO_2 gas mixture inside MD box.
- MD outputs predicted the number of O_2 and CO_2 molecules which passed from graphene membrane are 652 (97.31% ratio) and 23 (32.86% ratio) molecules after t = 1 ns.
- Numerically, the permeability of graphene membrane reach to 77 L/cm^2/day/MPa value by atomic structure optimization.
- Increasing of graphene atomic layers distance in simulated membrane, cause the accuracy improve and performance speed decrease in atomic purification process. Numerically, interaction energy between membrane and gas mixture converged to −32.09 eV by this atomic process done.
- Increasing of graphene atomic layers porous, cause the accuracy decrease and performance speed increase in atomic purification process. Numerically, interaction energy between membrane and gas mixture converged to −49.93 eV by this atomic process done.

These MD simulation results was shown that, the atomic arrangement of carbon atoms in graphene-based membrane can be improve the purification process accuracy or speed. Practically, these estimated results can be implemented in various purification process to optimize the industrial application efficiency.

Author contributions

Conceptualization, MPP and BPA; methodology, MPP and BPA; software, MPP and BPA; validation, MPP and BPA; formal analysis, MPP and BPA; investigation, MPP and BPA; resources, MPP and BPA; data curation, MPP and BPA; writing—original draft preparation, MPP and BPA; writing—review and editing, RS; visualization, MPP and BPA; supervision, RS; project administration, RS; funding acquisition, RS. All authors have read and agreed to the published version of the manuscript.

Conflict of interest

The authors declare no conflict of interest.

Nomenclature

F_{ij}	Atomic force between i and j atoms;
V_{ij}	Potential energy between i and j atoms;
m	Atomic mass;
r_c	Cut-off radius;
r_{ij}	Distance between i and j atoms;
t	Time step in molecular dynamics simulation;
T	Temperature in molecular dynamics simulation;
v	Atomic velocity;
N_{atom}	Number of atoms;
N_{sf}	Degree of freedom;
k_B	Boltzman constant;
r_0	Equilibrium bond length;
ε	Energy constant in Lennard-Jones function;
σ	Length constant in Lennard-Jones function;
θ_0	Equilibrium angle.

References

1. Bunch JS, Verbridge SS, Alden JS, et al. Impermeable Atomic Membranes from Graphene Sheets. Nano Letters. 2008; 8(8): 2458-2462. doi: 10.1021/nl801457b
2. Gilje S, Han S, Wang M, et al. A Chemical Route to Graphene for Device Applications. Nano Letters. 2007; 7(11): 3394-3398. doi: 10.1021/nl0717715
3. Schniepp HC, Li JL, McAllister MJ, et al. Functionalized Single Graphene Sheets Derived from Splitting Graphite Oxide. The Journal of Physical Chemistry B. 2006; 110(17): 8535-8539. doi: 10.1021/jp060936f
4. Zhou F, Fathizadeh M, Yu M. Single- to Few-Layered, Graphene-Based Separation Membranes. Annual Review of Chemical and Biomolecular Engineering. 2018; 9(1): 17-39. doi: 10.1146/annurev-chembioeng-060817-084046
5. Geim AK, Novoselov KS. The rise of graphene. Nature Materials. 2007; 6(3): 183-191. doi: 10.1038/nmat1849
6. Peres NMR, Ribeiro RM. Focus on graphene. New Journal of Physics. 2009; 11(9): 095002. doi: 10.1088/1367-2630/11/9/095002
7. Boehm HP, Setton R, Stumpp E. Nomenclature and terminology of graphite intercalation compounds (IUPAC Recommendations 1994). Pure and Applied Chemistry. 1994; 66(9): 1893-1901. doi: 10.1351/pac199466091893
8. Harris P. Transmission Electron Microscopy of Carbon: A Brief History. C. 2018; 4(1): 4. doi: 10.3390/c4010004
9. Nair RR, Blake P, Grigorenko AN, et al. Fine Structure Constant Defines Visual Transparency of Graphene. Science. 2008; 320(5881): 1308-1308. doi: 10.1126/science.1156965
10. Lee C, Wei X, Kysar JW, et al. Measurement of the Elastic Properties and Intrinsic Strength of Monolayer Graphene. Science. 2008; 321(5887): 385-388. doi: 10.1126/science.1157996
11. Tsang ACH, Kwok HYH, Leung DYC. The use of graphene based materials for fuel cell, photovoltaics, and supercapacitor electrode materials. Solid State Sciences. 2017; 67: A1-A14. doi: 10.1016/j.solidstatesciences.2017.03.015
12. Qu L, Liu Y, Baek JB, et al. Nitrogen-Doped Graphene as Efficient Metal-Free Electrocatalyst for Oxygen Reduction in Fuel Cells. ACS Nano. 2010; 4(3): 1321-1326. doi: 10.1021/nn901850u
13. Vivekchand SRC, Rout CS, Subrahmanyam KS, et al. Graphene-based electrochemical supercapacitors. Journal of Chemical Sciences. 2008; 120(1): 9-13. doi: 10.1007/s12039-008-0002-7
14. Zhang LL, Zhou R, Zhao XS. Graphene-based materials as supercapacitor electrodes. Journal of Materials Chemistry. 2010; 20(29): 5983. doi: 10.1039/c000417k
15. Li H, Zou L, Pan L, et al. Novel Graphene-Like Electrodes for Capacitive Deionization. Environmental Science & Technology. 2010; 44(22): 8692-8697. doi: 10.1021/es101888j
16. Zhang D, Yan T, Shi L, et al. Enhanced capacitive deionization performance of graphene/carbon nanotube composites. Journal of Materials Chemistry. 2012; 22(29): 14696. doi: 10.1039/c2jm31393f
17. Yin H, Zhao S, Wan J, et al. Three-Dimensional Graphene/Metal Oxide Nanoparticle Hybrids for High‐Performance Capacitive Deionization of Saline Water. Advanced Materials. 2013; 25(43): 6270-6276. doi: 10.1002/adma.201302223
18. Cohen-Tanugi D, Grossman JC. Water Desalination across Nanoporous Graphene. Nano Letters. 2012; 12(7): 3602-3608. doi: 10.1021/nl3012853
19. You Y, Sahajwalla V, Yoshimura M, et al. Graphene and graphene oxide for desalination. Nanoscale. 2016; 8(1): 117-119. doi: 10.1039/c5nr06154g
20. Cohen-Tanugi D, Lin LC, Grossman JC. Multilayer Nanoporous Graphene Membranes for Water Desalination. Nano Letters. 2016; 16(2): 1027-1033. doi: 10.1021/acs.nanolett.5b04089
21. Xue C, Wang X, Zhu W, et al. Electrochemical serotonin sensing interface based on double-layered membrane of reduced graphene oxide/polyaniline nanocomposites and molecularly imprinted polymers embedded with gold nanoparticles. Sensors and Actuators B: Chemical. 2014; 196: 57-63. doi: 10.1016/j.snb.2014.01.100
22. Asgari A, Nguyen Q, Karimipour A, et al. Investigation of additives nanoparticles and sphere barriers effects on the fluid flow inside a nanochannel impressed by an extrinsic electric field: A molecular dynamics simulation. Journal of Molecular Liquids. 2020; 318: 114023. doi: 10.1016/j.molliq.2020.114023
23. Ashkezari AZ, Jolfaei NA, Jolfaei NA, et al. Calculation of the thermal conductivity of human serum albumin (HSA) with equilibrium/non-equilibrium molecular dynamics approaches. Computer Methods and Programs in Biomedicine. 2020; 188: 105256. doi: 10.1016/j.cmpb.2019.105256
24. Ghanbari A, Warchomicka F, Sommitsch C, et al. Investigation of the Oxidation Mechanism of Dopamine Functionalization in an AZ31 Magnesium Alloy for Biomedical Applications. Coatings. 2019; 9(9): 584. doi: 10.3390/coatings9090584

25. Sabetvand R, Ghazi ME, Izadifard M. Studying temperature effects on electronic and optical properties of cubic CH3NH3SnI3 perovskite. Journal of Computational Electronics. 2020; 19(1): 70-79. doi: 10.1007/s10825-020-01443-3
26. Cohen-Tanugi D, Grossman JC. Water Desalination across Nanoporous Graphene. Nano Letters. 2012; 12(7): 3602-3608. doi: 10.1021/nl3012853
27. Cohen-Tanugi D, Lin LC, Grossman JC. Multilayer Nanoporous Graphene Membranes for Water Desalination. Nano Letters. 2016; 16(2): 1027-1033. doi: 10.1021/acs.nanolett.5b04089
28. Kim HW, Yoon HW, Yoon SM, et al. Selective Gas Transport Through Few-Layered Graphene and Graphene Oxide Membranes. Science. 2013; 342(6154): 91-95. doi: 10.1126/science.1236098
29. Wang J, Zhang P, Liang B, et al. Graphene Oxide as an Effective Barrier on a Porous Nanofibrous Membrane for Water Treatment. ACS Applied Materials & Interfaces. 2016; 8(9): 6211-6218. doi: 10.1021/acsami.5b12723
30. Plimpton S. Fast Parallel Algorithms for Short-Range Molecular Dynamics. Journal of Computational Physics. 1995; 117(1): 1-19. doi: 10.1006/jcph.1995.1039
31. Plimpton SJ, Thompson AP. Computational aspects of many-body potentials. MRS Bulletin. 2012; 37(5): 513-521. doi: 10.1557/mrs.2012.96
32. Aktulga HM, Fogarty JC, Pandit SA, et al. Parallel reactive molecular dynamics: Numerical methods and algorithmic techniques. Parallel Computing. 2012; 38(4-5): 245-259. doi: 10.1016/j.parco.2011.08.005
33. Brown WM, Wang P, Plimpton SJ, et al. Implementing molecular dynamics on hybrid high performance computers – short range forces. Computer Physics Communications. 2011; 182(4): 898-911. doi: 10.1016/j.cpc.2010.12.021
34. Stukowski A. Visualization and analysis of atomistic simulation data with OVITO–the Open Visualization Tool. Modelling and Simulation in Materials Science and Engineering. 2009; 18(1): 015012. doi: 10.1088/0965-0393/18/1/015012
35. Rapaport DC. The Art of Molecular Dynamics Simulation, 2nd ed. Cambridge University Press; 2004.
36. Nosé S. A unified formulation of the constant temperature molecular dynamics methods. The Journal of Chemical Physics. 1984; 81(1): 511-519. doi: 10.1063/1.447334
37. Hoover WG. Canonical dynamics: Equilibrium phase-space distributions. Physical Review A. 1985; 31(3): 1695-1697. doi: 10.1103/physreva.31.1695
38. Mayo SL, Olafson BD, Goddard WA. DREIDING: a generic force field for molecular simulations. The Journal of Physical Chemistry. 1990; 94(26): 8897-8909. doi: 10.1021/j100389a010
39. Tersoff J. New empirical approach for the structure and energy of covalent systems. Physical Review B. 1988; 37(12): 6991-7000. doi: 10.1103/physrevb.37.6991
40. Lennard-Jones JE. On the Determination of Molecular Fields. Proceedings of the Royal Society of London. 1924; 106(738): 463–477.
41. Cohen-Tanugi D, Grossman JC. Water permeability of nanoporous graphene at realistic pressures for reverse osmosis desalination. The Journal of Chemical Physics. 2014; 141(7). doi: 10.1063/1.4892638
42. Nair RR, Wu HA, Jayaram PN, et al. Unimpeded Permeation of Water Through Helium-Leak–Tight Graphene-Based Membranes. Science. 2012; 335(6067): 442-444. doi: 10.1126/science.1211694